Journal of the American College of Cardiology
© 2008 by the American College of Cardiology Foundation
Published by Elsevier Inc.

Vol. 51, No. 4, 2008
ISSN 0735-1097/08/$34.00
doi:10.1016/j.jacc.2007.07.093

PRECLINICAL RESEARCH

Mitral Regurgitation Augments Post-Myocardial Infarction Remodeling

Failure of Hypertrophic Compensation

Ronen Beeri, MD,* Chaim Yosefy, MD,* J. Luis Guerrero, BS,* Francesca Nesta, MD,* Suzan Abedat, MSc,§ Miguel Chaput, MD,* Federica del Monte, MD, PhD,† Mark D. Handschumacher, BS,* Robert Stroud, MS,‖ Suzanne Sullivan, BS,* Thea Pugatsch, PhD,§ Dan Gilon, MD, FACC,§ Gus J. Vlahakes, MD, FACC,‡ Francis G. Spinale, MD, FACC,‖ Roger J. Hajjar, MD, FACC,† Robert A. Levine, MD, FACC*

Boston, Massachusetts; Jerusalem, Israel; and Charleston, South Carolina

Objectives We examined whether mitral regurgitation (MR) augments post-myocardial infarction (MI) remodeling.

Background MR doubles mortality after MI, but its additive contribution to left ventricular (LV) remodeling is debated and has not been addressed in a controlled fashion.

Methods Apical MIs were created in 12 sheep, and 6 had an LV-to-left atrial shunt implanted, consistently producing regurgitant fractions of ~30%. The groups were compared at baseline, 1, and 3 months.

Results Left ventricular end-systolic volume progressively increased by 190% with MR versus 90% without MR ($p < 0.02$). Pre-load–recruitable stroke work declined by 82 ± 13% versus 25 ± 16% ($p < 0.01$) with MR, with decreased remote-zone sarcoplasmic reticulum Ca^{2+}-ATPase levels (0.56 ± 0.03 vs. 0.76 ± 0.02, $p < 0.001$), and decreased isolated myocyte contractility. In remote zones, pro-hypertrophic Akt and gp130 were upregulated in both groups at 1 month, but significantly lower and below baseline in the MR group at 3 months. Pro-apoptotic caspase 3 remained high in both groups. Matrix metalloproteinase (MMP)-13 and membrane-type MMP-1 were increased in remote zones of MR versus infarct-only animals at 1 month, then fell below baseline. The MMP tissue inhibitors rose from baseline to 3 months in all animals, rising higher in the MI + MR–group border zone.

Conclusions In this controlled model, moderate MR worsens post-MI remodeling, with reduced contractility. Pro-hypertrophic pathways are initially upregulated but subsequently fall below infarct-only levels and baseline; with sustained caspase 3 elevation, transformation to a failure phenotype occurs. Extracellular matrix turnover increases in MR animals. Therefore, MR can precipitate an earlier onset of dilated heart failure. (J Am Coll Cardiol 2008;51:476–86) © 2008 by the American College of Cardiology Foundation

Expansion of infarcted tissue begins acutely after myocardial infarction (MI). A more gradual remodeling process, however, also involves the noninfarcted areas (1,2); initially compensatory, this process subsequently becomes maladaptive, generating a larger, more spherical, and poorly contracting ventricle (3–7), associated with reduced survival (2,8,9).

See page 487

Myocardial infarction can also cause mitral regurgitation (MR) by altering ventricular geometry and function (10–12). Such ischemic MR doubles the risk of death after MI (13,14). Severe nonischemic MR has been shown to promote left ventricular (LV) remodeling and reduce survival (15–19). However, whether more typically moderate ischemic MR does so remains controversial. A recent paper maintained that "ischemic MR is a consequence, not a cause, of post-infarction remodeling," because remodeling persisted despite annuloplasty with apparent MR reduction

From the *Cardiac Ultrasound Laboratory, †Cardiovascular Research Center, and ‡Cardiac Surgery Department, Massachusetts General Hospital and Harvard Medical School, Boston, Massachusetts; §Heart Institute and Cardiovascular Research Laboratory, Hadassah-Hebrew University Medical Center, Jerusalem, Israel; and the ‖Cardiothoracic Surgery Department, Medical University of South Carolina, Charleston, South Carolina. Supported, in part, by a Grant-in-Aid (0350422N) of the American Heart Association; grants R01HL38176, R01HL72265, and K24HL67434 from the NIH/NHLBI; and a grant from the USA-Israel Binational Science Foundation (no. 2001037).

Manuscript received May 3, 2007; revised manuscript received July 9, 2007, accepted July 16, 2007.

(20). Practically, "MR might not represent a target for therapy if indeed it is not the major culprit" (21), adding to the uncertainty regarding the risk versus benefit of repairing ischemic MR (22).

In patients, ischemic myocardial changes and regurgitation develop concurrently, precluding the ability to separate their effects and analyze their interaction directly (23). This requires a model in which MR can be varied independently in the presence of MI, but without interventions such as infarct patching (24–27) that might themselves influence remodeling. Most experimental studies of post-MI remodeling have used an infero-posterior MI model (27,28); this has the disadvantage of linking the MI-induced remodeling to the development of MR. We therefore tested the incremental contribution of MR in a controlled manner using a model in which the MI by itself does not cause MR, and the MR can be created in a standardized and fixed fashion (29,30).

In such a study, it must be recalled that remodeling is a complex process, involving changes not only in ventricular geometry (3) and in global and regional myocardial function (31), but also in calcium handling, molecular signals promoting hypertrophy, cardiomyocyte viability (32–34), and extracellular matrix turnover (35). Intracellular pathways that promote compensatory hypertrophy also tend, if chronically activated, to drive cells down pathways to cell death by apoptosis and thus to loss of contractile elements, with further deterioration of cardiac function (Fig. 1). Accordingly, it is important to correlate evidence of remodeling at the molecular, cellular, and whole-heart levels (36). We therefore tested the hypothesis that MR accompanying MI produces greater remodeling than a comparable infarct alone, and may be associated with a different progression of molecular events, with transition from signals promoting hypertrophy to those inducing failure.

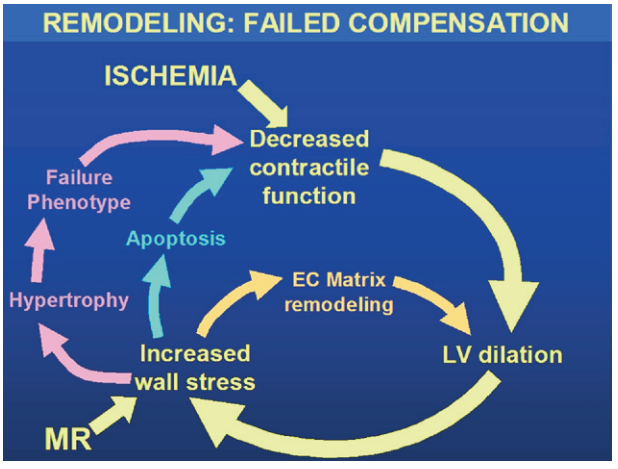

Figure 1 The Vicious Cycle of Remodeling

EC = extracellular; LV = left ventricle; MR = mitral regurgitation.

Methods

MR model. A modification of the chronic MR sheep model of Rankin et al. (29) was implemented in conjunction with Luis Guerrero, a surgeon experienced in physiological modeling, using an 8-cm long, 8-mm diameter reinforced Teflon (PTFE) graft (Edwards Lifesciences, Irvine, California) (cross-sectional area of 0.50 cm^2) implanted under sterile conditions into the LV base and left atrial (LA) appendage with intramuscular portions stiffened with epoxy resin (Fig. 2). The regurgitant flow was confirmed during each thoracotomy (see the following text) using a transonic flow probe and color Doppler echocardiography imaging. The standardized shunt diameter and length have produced consistent levels of MR (regurgitant fractions of approximately 30%, corresponding to moderate MR [37]). Animals were treated with heparin (3 days) and then oral aspirin.

Abbreviations and Acronyms

- **EF** = ejection fraction
- **LA** = left atrium/atrial
- **LV** = left ventricle/ventricular
- **MI** = myocardial infarction
- **MMP** = matrix metalloproteinase
- **MR** = mitral regurgitation
- **MT-MMP** = membrane-type matrix metalloproteinase
- **SERCA2a** = sarcoplasmic reticulum Ca^{2+}-ATPase
- **TIMP** = tissue inhibitor of matrix metalloproteinase
- **2D** = 2-dimensional
- **3D** = 3-dimensional

Animal studies. A total of 12 Dorsett hybrid sheep (20 to 30 kg) were loaded for 3 days with amiodarone (200 mg orally twice a day) then anesthetized with thiopentothal sodium (0.5 ml/kg), intubated, and ventilated at 15 ml/kg with a 2% isoflurane-oxygen mixture. All received glycopyrrolate (0.4 mg intravenously) and prophylactic vancomycin (0.5 g intravenously) and amiodarone (150 mg intravenous drip over the course of the operation). Surface electrocardiogram (ECG) was monitored, and a sterile left thoracotomy performed with pericardial incision and creation of a cradle. A high-fidelity micromanometer-tipped catheter (Millar Instruments Inc., Houston, Texas) was placed into the LV. After baseline 2-dimensional (2D) and 3-dimensional (3D) echocardiography imaging, an anteroapical MI was produced by ligating the mid- to distal left anterior descending coronary artery, known to produce a substantial MI without MR (38). An immediate 2D echocardiography apical image was performed to confirm that septal wall motion abnormality extended approximately one-third of the way from LV apex to base for standardization. Mitral regurgitation equivalent volume overload was created for 90 days in 6 sheep with an open LV-to-LA shunt (referred to as the infarct + MR group); in the other 6, the shunt was closed (infarct-only group). In addition to analgesia, propranolol, 1 mg intravenously in 2 divided doses, was given for evident stress and sinus tachycardia (>150) upon extubation. Antibiotics (cephapirin, 0.5 g intravenously) and analgesics (buprenorphine, 0.3 mg twice a day) were administered for the next 5 days, and oral amiodarone (200 mg twice a day) for the next 3.

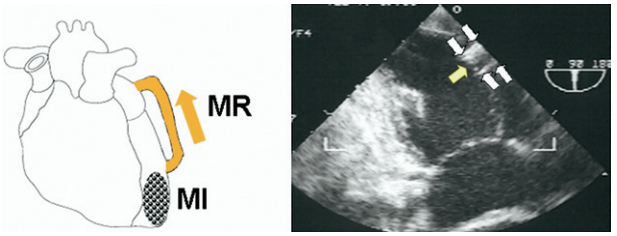

Figure 2 **Schematic and 2D Echocardiographic Image of the LA-LV Shunt Creating MR**

Single arrows indicate flow direction; **paired arrows** indicate shunt exit from the LV. LA = left atrial; MI = myocardial infarction; 2D = 2-dimensional; other abbreviations as in Figure 1.

During repeat sterile thoracotomy at day 30, 3D echocardiography was performed to evaluate LV remodeling and function, with directed biopsies of the noninfarcted myocardium near and remote from the border zone using a TruCut needle (Cook, Winston-Salem, North Carolina). At day 90, 3D echocardiography and blood sampling were repeated at thoracotomy, followed by euthanasia and whole-heart pathological and myocyte size and contractility studies that require considerable tissue. The animal studies conformed to National Institutes of Health Guidelines for Animal Research (Guide for the Care and Use of Laboratory Animals, National Research Council, Washington, DC, 1996) and were approved by the institutional animal care committee.

3D echocardiography and LV function. Three-dimensional quantitation is necessary because LV shape changes with chronic MR, as well as MI (39). Rotated apical images were obtained at 10° intervals with an epicardial 5-MHz transesophageal echocardiography probe (Sonos 7500, Philips Medical Systems, Andover, Massachusetts), rotated by software and gated to ECG and respiration. Digital images were analyzed on a workstation with custom programs (40). Endocardial surfaces were traced to calculate LV volumes and ejection fraction (EF), and coded for wall motion abnormality to produce a quantitative 3D wall motion map validated against a 36-crystal sonomicrometer array (41). Remodeling was quantified in terms of increasing LV volumes (42). Regurgitant fraction was calculated as transonic MR-equivalent flow divided by LV ejection volume, with cross-correlation by pulsed Doppler time–velocity integral of shunt flow multiplied by shunt cross-sectional area. At thoracotomy, the initial and final pressure–volume loops were obtained using Millar catheters and 4 sterile subendocardial crystals (Sonometrics Corp., London, Ontario, Canada), with an inferior vena cava occlusion to obtain the end-systolic pressure–volume relation for contractility (43) and pre-load–recruitable stroke work (44). Crystals were located at the LV apex and base (between aorta and mitral annulus) and anteriorly and posteriorly along a midventricular short-axis. Crystals were not placed at day 30 to maximize sterility and survival. dP/dt was obtained by the high-fidelity Millar catheter (Millar Instruments, Houston, Texas).

Myocyte size and contraction. Small (5 to 10 g) areas of tissue were removed at euthanasia from the noninfarcted LV and perfused via the corresponding coronary artery for 5 min with low-magnesium Krebs-Henseleit (KH) cardioplegia solution. Myocardial cells were isolated using a well-established method (45,46). The LV sections were perfused with Ca^{2+}-free KH containing collagenase (Worthington Biochem Corp., Lakewood, New Jersey) and hyaluronidase (Sigma, St. Louis, Missouri). Ventricular muscle tissue was minced into small pieces and placed in enzyme buffer I (Sigma) in the presence of trypsin and deoxy-ribonuclease. The tissue was washed in a 3:1 mixture of Ca^{2+}-free KH in Dulbecco's phosphate-buffered saline (GIBCO, Gaithersburg, Maryland). Cells were loaded with the Ca^{2+} fluorescent indicator Fura-2 for 15 min in a light-sealed chamber mounted on an inverted microscope. Myocyte length and width were measured offline on 50 consecutive cells using commercial image analysis software to establish proportions of normal short cells versus elongated cells characteristic of eccentric hypertrophy in the failing phenotype. The cells were excited to contract using platinum electrodes in the bath, and a dual excitation spectrofluorometer recorded fluorescence emissions (505 nm from exciting wavelengths 340 mm and 380 mm) to calculate intracellular calcium concentrations. Cell motion was measured by a video-edge motion detector (Crescent Electronics, Sandy, Utah) (45).

Molecular assays. We measured levels of several molecular species that determine cell contractility, that modulate cell hypertrophy and death, and that are responsible for extracellular matrix turnover. All protein assays were performed and specimens pooled from the same treatment group and stage.

Calcium cycling proteins: sarcoplasmic reticulum Ca^{2+}-ATPase (SERCA2a) and phospholamban. Sarcoplasmic reticulum membranes were obtained from the myocardial biopsy specimens using a sucrose gradient centrifugation method (47). Myocardium was homogenized and centrifuged at 7,700 *g* for 20 min, and the supernatant filtered and centrifuged at 136,000 *g* for 60 min. The pellets, resuspended and rehomogenized in 10% sucrose buffer, were centrifuged at 55,000 *g* in a 10% to 40% sucrose gradient, and the bands between 30% and 40% enriched in sarcoplasmic reticulum were collected, centrifuged at 136,000 *g* for 60 min, and the pellet resuspended in freezing buffer. Protein was determined by a modified Bradford procedure (using bovine serum albumin for the standard curve). Proteins were separated from the sarcoplasmic reticulum vesicle preparation from tissue frozen in liquid nitrogen, and an immunoblot using monoclonal anti-SERCA2 and phospholamban performed. Proteins levels were normalized against total myocardial protein.

Pro-hypertrophic and anti-apoptotic cascades. We measured levels of Akt (protein kinase B) and gp130, which are

both at their respective levels (cytosol and membrane) important crossroads in pro-hypertrophic signaling; and caspase 3, the final common pathway for intracellular signaling of apoptosis. Western blot analysis was performed on cell lysates from biopsies at baseline and days 30 and 90. Antibodies binding for anti-gp130, anti-phospho Akt, and antiactivated caspase 3 (48) were detected with a peroxidase-conjugated antimouse IgG and chemiluminescence. α-Actin was used as a housekeeping control. Densitometry of the blots was assessed using commercially available software (Photoshop 5, Adobe Systems Inc., San Jose, California).

Modulators of extracellular matrix turnover: matrix metalloproteinases (MMPs). Assays were performed for membrane-type matrix metalloproteinase-1 (MT1-MMP), MMP-13, tissue inhibitor of matrix metalloproteinase (TIMP)-1, and TIMP-4 by immunoblotting using methods previously described (35). Left ventricular myocardial samples were homogenized and concentrated to prevent MMP proteolytic activation and degradation. Trypsin (2.5 μM; 5 min) was used to cleave nascent MMPs to fully activate enzyme moieties and/or facilitate the removal of endogenous inhibitors. Relative TIMP-1, TIMP-4, MT1-MMP, and MMP-13 levels were then measured by immunoblotting. A positive control was included in all immunoblots (MMP-13: CC068; MT1-MMP: CC1042) (Chemicon, Temecula, California).

Statistics. Statistical analysis was performed using a Student *t* test for continuous variables and a chi-square test for categorical variables (Stat View 5, SAS Institute Inc., Cary, North Carolina). A value of $p < 0.05$ was considered significant. Multiple comparisons were performed using analysis of variance (for repeated measurement where needed) and a Student-Neumann Keuls post-hoc test. Interobserver and intraobserver variability for 3D echo-measured LV volumes and EF in our laboratory is 3.5%.

Results

Remodeling: LV volumes. Left ventricular end-diastolic volume relative to the acute post-MI value increased by an average of 26% in the infarct-only group versus 130% in those with volume overload ($p < 0.02$). Left ventricular end-systolic volume progressively increased by 190% with MR-type volume overload versus 90% with MI only ($p < 0.02$) (Figs. 3 and 4).

Remodeling: LV function. Pre-load–recruitable stroke work from pressure-volume loops declined more in the infarct + MR group by 82 ± 13% versus 25 ± 16% of baseline in the infarct-only group ($p < 0.01$). Left ventricular dP/dt also declined progressively in the MR group to 52 ± 9% of baseline, but only by 22 ± 12% in the shams ($p < 0.04$) (Fig. 4). These results were corroborated by reduced contractility of isolated cells with reduced calcium transients and increased diastolic intracellular calcium concentration (Tables 1 and 2). The diastolic relaxation constant *tau* was more prolonged in the infarct + MR group (78 ± 23 ms vs. 44 ± 13 ms, $p < 0.01$).

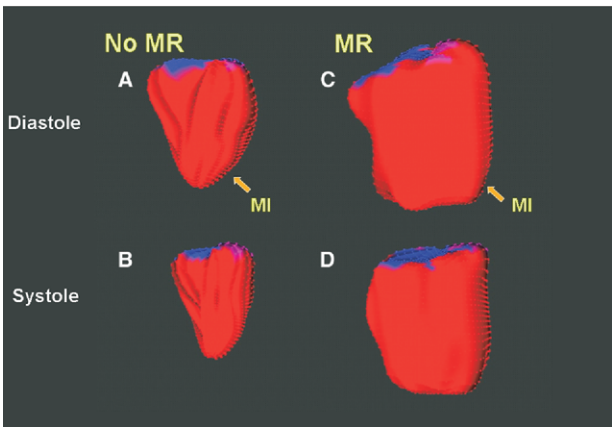

Figure 3 **Echocardiographic 3D Reconstructions of the Endocardial Surface of the LV**

Echocardiographic 3-dimensional (3D) reconstructions of the endocardial surface of infarct (MI) only **(A and B)** and infarct + MR **(C and D)** animals at diastole **(top)** and systole **(bottom)**. Note the enlarged and spherical infarct + MR ventricles. Abbreviations as in Figures 1 and 2.

Calcium cycling proteins. As shown in Figure 5, SERCA2a abundance was downregulated in the infarct region and border zone compared with the remote region in both infarct + MR and infarct-only sheep LVs. There was a lower level of SERCA2a in the remote zone of infarct + MR than of infarct-only sheep. Phospholamban was unchanged in all regions. These changes are typical for remodeling myocardium.

Intracellular signaling pathways. Akt, a pro-hypertrophic enzyme (49), was upregulated in the remote zones of infarct + MR and infarct-only animals at 1 month, but was lower in animals with than without MR at 3 months (Fig. 6). In the infarct + MR group at 3 months, Akt also fell below baseline of the same group. The same pattern was observed for the interleukin-6-family receptor subunit gp130 (50). Expression of activated caspase 3 (32–34,51), the final common pathway of apoptosis, remained elevated in all regions of both groups at both 1 and 3 months.

Cell morphology. Myocytes in the MR group were elongated, characteristic of myocardial failure (45), compared with cells from the MI-only animals (Fig. 7).

Extracellular matrix and MMPs. In the remote myocardium of infarct + MR sheep, at initial follow-up, there was a significant increase in MMP-13 and MT1-MMP, followed by a decrease at the time of sacrifice (Fig. 8, "shunt remote" bars): MMP-13 increased to 238 ± 29% of baseline at follow-up, and then fell to 79 ± 13% of baseline at 3 months sacrifice; MT1-MMP increased to 165 ± 23% of baseline at follow-up, and then fell to 85 ± 16% of baseline at sacrifice. In the remote myocardium of infarct-only sheep, the rise and fall of MMP-13 did not reach statistical

JACC Vol. 51, No. 4, 2008
January 29, 2008:476–86

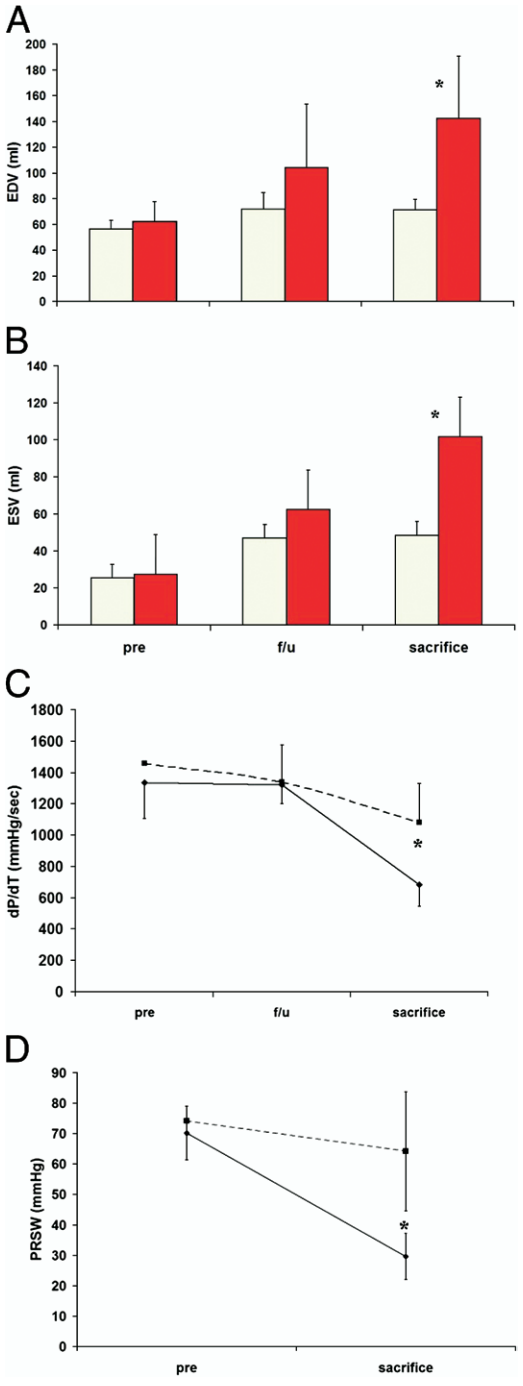

Figure 4 Measurement of LV Volumes and Function

End-diastolic volume (EDV) **(A)** and end-systolic volume (ESV) **(B)** of infarct-only **(yellow bars)** and infarct + MR **(red bars)** sheep at baseline (pre), 1 month follow-up (f/u), and 3 months sacrifice. **(C and D)** dP/dt and pre-load–recruitable stroke work (PRSW) of infarct-only **(broken lines)** and infarct + MR **(solid lines)** sheep at pre, f/u, and 3 months sacrifice. *p < 0.05. Abbreviations as in Figure 1.

significance (170 ± 85% of baseline at initial follow-up; 75 ± 22% at sacrifice), and MT1-MMP did not significantly increase at 1 month (Fig. 8, "sham remote" bars). In the border zones of the infarct-only sheep, there was a significant decrease in MT1-MMP at sacrifice (to 60 ± 8% of baseline), with levels maintained in the infarct + MR group. In contrast, TIMP-4 showed progressive rises from baseline to initial follow-up and then to sacrifice in the border and remote zones of both groups, with significantly higher levels at sacrifice in the infarct + MR group border zone (207 ± 9% vs. 152 ± 10% of baseline, $p < 0.05$). Tissue inhibitor of matrix metalloproteinase-1 showed a similar pattern of progressive increases in the infarct + MR group remote zone, with a significant late rise at sacrifice.

Table 1 Isolated Cardiomyocyte Contractility in the Different Groups

Contractility Measurements	Normal Control Sheep	Infarct + MR	Infarct Only
Cell shortening (%)	5.7 ± 0.4	2.6 ± 0.7*	3.5 ± 0.3*†
t90% (ms)	390 ± 82	676 ± 68*	510 ± 59*†

*p < 0.01 compared with normal control sheep; †p < 0.01 compared with infarct + mitral regurgitation (MR) group.
t90% = time to 90% relaxation.

Discussion

Myocardial infarction, with loss of contracting myocytes, leads to a sequence of events aimed at preserving cardiac output, including increased LV end-diastolic volume to augment pre-load. Cells in noninfarcted areas hypertrophy by addition of contractile elements in series, creating eccentric hypertrophy without increased wall thickness. This allows the LV to dilate, a process that is also promoted by altered MMP activation with extracellular matrix degradation (52), and acceleration of cell death by apoptosis (32,53). This process eventually culminates in systolic enlargement, extensive fibrosis, and LV failure, the extent of which predicts further cardiac events (2,9). Volume and pressure overload increase wall stress, which can aggravate remodeling (54) and promote eccentric hypertrophy through increased fiber stretch (Fig. 1). Conversely, hemodynamically unloading the LV reverses the functional and cellular stigmata of cardiac failure as well as the remodeling process (55,56). Neurohumoral activation and activation of inflammatory mediators and cytokines initially compensate for reduced cardiac output but, in the long term, mediate increased load, cell death, and cardiac fibrosis (50,57–59). Increased wall stress also up-regulates the production and

Table 2 Intracellular Calcium Measurements in the Different Groups

Calcium Measurements	Normal Control Sheep	Infarct + MR	Infarct Only
Diastolic (Ca^{2+}) (nM)	230 ± 41	320 ± 21*	275 ± 22*†
Systolic (Ca^{2+}) (nM)	796 ± 24	535 ± 44*	714 ± 43*‡
t90% (ms)	361 ± 34	542 ± 38*	455 ± 43*†

*p < 0.01 compared with normal control sheep; †p < 0.03 compared with infarct + mitral regurgitation (MR) group; ‡p < 0.005 compared with infarct + MR group.
t90% = time to 90% relaxation of the calcium signal.

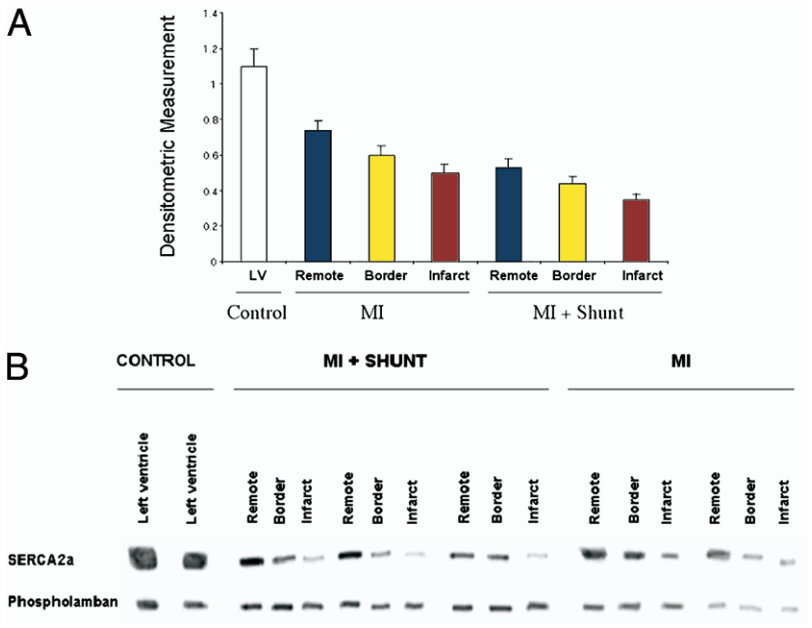

Figure 5 **SERCA2a and Phospholamban Quantification**

(A) Quantification of sarcoplasmic reticulum Ca^{2+}-ATPase (SERCA2a) activity in remote, border, and infarct regions of experimental and normal control sheep hearts. **(B)** Immunoblots from different regions of the myocardium in different groups for SERCA2a and phospholamban. Note that in the infarct region, there was residual myocardium that was homogenized and protein extracted. Abbreviations as in Figures 1 and 2.

release of MMPs, which are believed to be pivotal in altering the extracellular matrix in ways that promote ventricular dilatation (60). Their transgenic activation induces congestive heart failure (61), and their inhibition attenuates post-MI remodeling (62,63).

Mitral regurgitation, caused by alterations in ventricular geometry and function after MI (10,12), can itself initiate the remodeling cascade, and causes progressive deterioration of ventricular function at a cellular and molecular level (15–17). Mitral regurgitation considerably alters the load on the LV. It increases diastolic wall stress, which can induce eccentric LV hypertrophy and subsequent dilatation and failure (18), and it thereby increases early systolic wall stress. Although MR permits LV emptying during systole into the lower-pressure LA, it has been shown actually to *increase* end-systolic wall stress and, hence, afterload in patients with chronic MR (64,65). Moreover, MR induces further LV dilatation due to activation of neurohumoral and cytokine components of the remodeling cascade (66–68). As MR is both a cause and a result of LV remodeling, it can potentially exacerbate the vicious cycle spiraling down to cardiac failure unless the remodeling or the MR is reversed (69–71).

Regarding clinical implications, knowing whether the parallel occurrence of MR and MI causes more pronounced remodeling is critical, because at least MR can be eliminated by repairing or replacing the valve, and thus relieving the volume overload induced by it. Separating these 2 dynamic processes in an experimental model is a challenge, because in most existing models they are linked. One recent study of inferior MIs, in fact, concluded that prevention of ischemic MR does not influence the outcome of remodeling (20), despite benefits in nonischemic models (18) and concerns in nonischemic patients (72). In our model, we therefore implanted an LV-to-LA shunt, which created a moderate and standardized MR-like regurgitant flow, independent of a medium-sized antero-apical MI that by itself does not cause MR.

In this controlled model, moderate MR worsened post-MI remodeling. Specifically, it induced large diastolic and systolic LV volumes reflecting volume overload and reduced global function. Reduced contractility was also apparent in less pre-load–dependent physiological measures such as pre-load–recruitable stroke work. These changes paralleled decreased single-cell contractility in the noninfarcted myocardium with reduced SERCA2a levels, which directly correlate with cell contraction (46).

In contrast to progressive changes in the LV, several mediators of the hypertrophic process underwent biphasic changes in the noninfarcted myocardium of animals with MR-type volume overload. These include gp130, a glycoprotein that forms heterodimers to produce different receptors, notably of the interleukin 6/CT1/LIF family. The activation of these receptors has been linked to cardiomyocyte hypertrophy (50,73), and their reduced abundance, manifested by reduced gp130 levels, has been associated with the transition from hypertrophy to failure (74,75). Akt, or protein kinase B, is a serine-threonine kinase activated by

JACC Vol. 51, No. 4, 2008
January 29, 2008:476–86

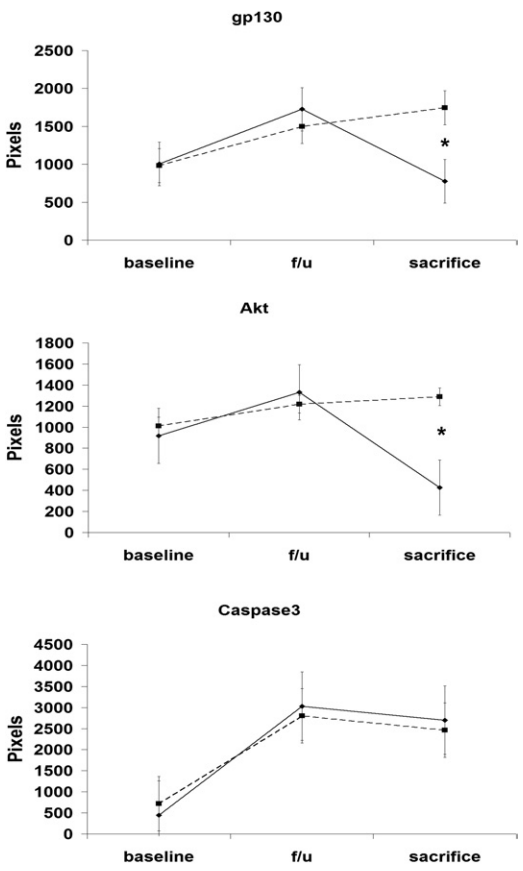

Figure 6 **Protein Levels of Akt, gp130, and Caspase 3**

Protein expression of Akt, gp130, and activated caspase 3 from infarct-only **(broken lines)** and infarct + mitral regurgitation **(solid lines)** sheep at baseline, 1 month follow-up (f/u), and 3 months sacrifice. Note the biphasic change in infarct + mitral regurgitation animals for gp130 and Akt expression at follow-up (high) and sacrifice, while no significant change is noted in caspase 3 levels. Values are ± standard error of the mean, *$p < 0.01$.

several pro-survival and -hypertrophic factors, among others cardiotrophin-1 (76), acting through the gp130-containing receptor, or growth factor receptors activating phosphoinositide-3 kinase (77).The constitutive activation of Akt in a model of rat ischemia-reperfusion injury reduced cell death and improved function (78). Like gp130, reduced levels of Akt are related to increased apoptosis and a transition from compensatory hypertrophy to a failure phenotype (49). In our model, while both infarct + MR and infarct-only sheep had elevated expression of Akt and gp130 after 1 month, the MR sheep demonstrated a notable reduction in these protein levels after 3 months, compared with the no-MR animals and with baseline. The pro-hypertrophic process, which begins in both groups at 1 month, continues in the animals without MR but is down-regulated at 3 months in the MR group, in association with continued adverse remodeling and LV dysfunction. This decline may represent earlier termination of the hypertrophic process or transition to a failure phenotype specific to the persistent-MR situation; either way, it represents failure of the hypertrophic process. The ongoing drive to cell death, with the suppressed pro-hypertrophic drive, further promotes the transition to failure. These findings are consistent with the emerging view of LV remodeling in general as a failed attempt at compensation for initial stresses on the myocardium—in this case, exacerbated by the MR volume overload (7,74); in others, it reflects the transition from hypertensive hypertrophy to failure (79,80).

There was also excessive activation of MMPs, notably MMP-13 and MT-MMP1, in the noninfarcted remote zone of the MR sheep. This could induce excess extracellular matrix turnover and potentially exacerbate remodeling. However, these same MMP levels fell at sacrifice, with the fall in remote-zone MT-MMP1 being significantly greater in the MR sheep, and the fall in MMP-13 being significant only for the MR group. As this change parallels the down-regulation of the pro-hypertrophic signaling process, it could be also part of the failure of compensation by limiting the adaptive geometrical changes in myocardial hypertrophy. Matrix metalloproteinase inhibitors showed a different pattern, with a progressive rise from baseline to sacrifice that was significantly greater with MR. This suggests a possible shift from matrix turnover to matrix accumulation and stabilization over time, a response typical of remodeling myocardium (81). However, it is clear that neither the MMP nor the TIMP changes adequately compensate for the remodeling process, as LV volume progressively rose while systolic function fell.

This study has several limitations. Ischemic MR affecting a native valve often progressively increases (28,69–71), but is inherently linked to the underlying MI and is not standardized. Based on the motivation for this study, it was

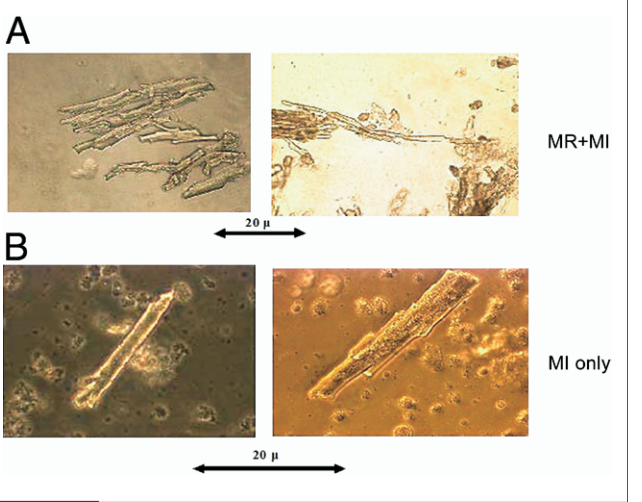

Figure 7 **Photomicrographs of Separated Cardiomyocytes**

Elongated myocytes from sheep with MI and MR shunt **(A)** versus more normal cells from MI-only animals **(B)**. Note the different scales used to accommodate the elongated cells of the MI + MR sheep within the field. Abbreviations as in Figures 1 and 2.

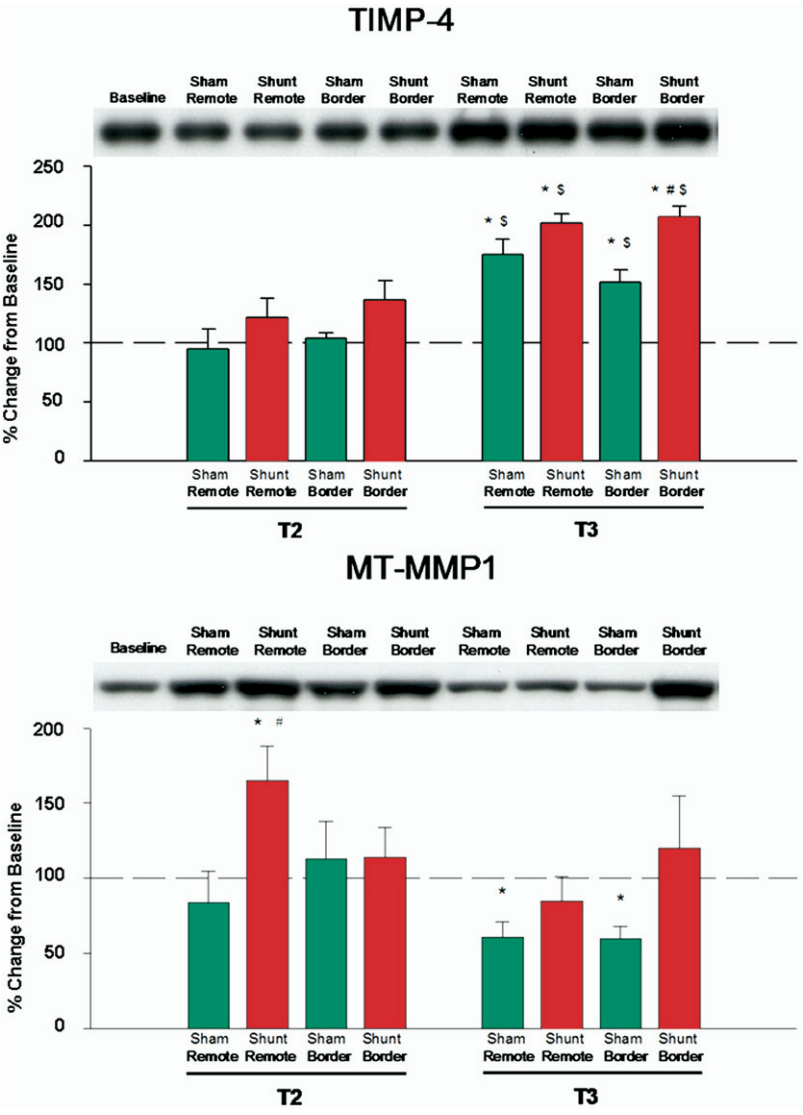

Figure 8 **MMP Abundance**

Levels of membrane-type (MT) matrix metalloproteinase (MMP)1 and tissue inhibitor of matrix metalloproteinase (TIMP)-4 in the infarct-only ("sham", **green bars**) and infarct + mitral regurgitation **(red bars)** animals at first follow-up (T2) and sacrifice (T3) time points. *$p < 0.05$ relative to baseline; #$p < 0.05$ for myocardial infarction + mitral regurgitation relative to myocardial infarction only animals for the same zone and stage; \$$p < 0.05$ for sacrifice relative to initial follow-up.

critical to separate the 2 processes of infarction and regurgitation to determine the incremental role of MR most directly, and to do so with a standardized orifice, which provided stable regurgitant fractions of ~30% throughout the study. Although the LV also fills through this valveless orifice, based on prior experience, this should not importantly alter LV filling (29).

We did not assess whether any one of the molecular changes reported in the present study is causative. We intended to test whether differences in remodeling based on MR are *associated* with molecular changes described in the remodeling process. Determining which factors are *causative* versus concomitants, and studying all possible factors, is beyond the scope of this study. Nevertheless, we analyzed pathways extensively linked to the pro-hypertrophic and remodeling processes, and causally implicated through transgenic and pharmacologic modification (61,74,78).

While the impact of isolated MR is important to explore, the study specifically addresses the challenge posed by the recent literature (20), which can be stated as an *alternative hypothesis* that remodeling in ischemic MR is caused only or predominantly by the underlying infarct, not the MR. This required comparing infarct-only versus infarct + MR groups. The data do show important effects of the infarct alone, with end-systolic volume nearly doubling, and increases in gp130, Akt, and caspase. The changes with infarct

plus MR, however, were greater, with end-systolic volume nearly tripling, and a different pattern of activation followed by exhaustion of hypertrophic- and apoptotic-signaling molecules gp130 and Akt. The findings, therefore, suggest *an additive rather than exclusive role of MR*. This is supported by our data (unpublished results) from sheep with an identical shunt and no MI, which did not cause significant remodeling in the same 3-month time-frame in terms of either volume or contractility changes.

Recently, contribution of MR to post-MI remodeling has been challenged by Guy et al. (20) in an inferior MI model in which either MR was reduced using an undersized annuloplasty ring repair, or MI was restrained using a mesh. The MR repair group remodeled more, leading to the suggestion that the MR is not causative, but may be a consequence of post-MI remodeling. The main caveat to these conclusions is that undersized ring annuloplasty may by itself alter LV mechanics, as recently shown (82), so as to exacerbate remodeling. Thus, the excess remodeling observed may have been caused, at least partially, by the repair itself, which was performed 2 weeks before infarct creation. The difficulty in eliminating MR as a potential contributor to continued remodeling by annuloplasty has also been reported (72). Another recent paper (83) has suggested that repairing MR in a subgroup of patients with LV dysfunction has no survival benefit. While this is intriguing, the patient population in that study had prominent LV dysfunction at baseline (<30% EF), and thus it is possible that repair was performed too late for many to benefit in terms of LV function or outcome. Based on their inclusion criteria, the patients also had at least moderate-to-severe MR—more severe than in our model. Further, unlike this MI model, roughly 40% of the patients did not have coronary artery disease as the basis for their LV dysfunction. Thus, these clinical data cannot readily be compared with our relatively mild MI model with normal baseline LV function and moderate MR. There is definitely a need for a randomized controlled study to clinically address the issue of mitral valve repair in moderate ischemic MR.

Conclusions

This study demonstrates that MR accompanying MI produces greater ventricular remodeling than a comparable infarction alone, with an earlier transition to a failure phenotype. This is the case even for only moderate MR, most typical of the ischemic situation, for which the greatest uncertainty exists regarding impact on the heart and need for intervention. The changes at the level of the whole heart parallel cellular and molecular abnormalities in the noninfarcted myocardium that reflect the complex remodeling process. These molecular events also progress differently with MR than with comparable infarction alone, with an initial rise in pro-hypertrophic and antiapoptotic signals, followed by their exhaustion. Recognizing this pattern can motivate a search for the responsible molecular "switch," so that decompensation might be limited or reversed, averting the earlier onset of dilated heart failure precipitated by MR that may portend a worse prognosis.

Reprint requests and correspondence: Dr. Robert A. Levine, Cardiac Ultrasound Laboratory YAW5, Massachusetts General Hospital, 55 Fruit Street, Boston, Massachusetts 02114. E-mail: rlevine@partners.org.

REFERENCES

1. Pfeffer MA, Braunwald E. Ventricular remodeling after myocardial infarction: experimental observations and clinical implications. Circulation 1990;81:1161–72.
2. Cohn JN, Ferrari R, Sharpe N. Cardiac remodeling—concepts and clinical implications: a consensus paper from an international forum on cardiac remodeling. J Am Coll Cardiol 2000;35:569–82.
3. Picard MH, Wilkins GT, Ray PA, Weyman AE. Progressive changes in ventricular structure and function during the year after acute myocardial infarction. Am Heart J 1992;124:24–31.
4. Pfeffer MA. Left ventricular remodeling after acute myocardial infarction. Annu Rev Med 1995;46:455–66.
5. Gianuzzi P, Temporelli PL, Bosimi E, et al., for the Gruppo Italiano per lo Studio della Sopravvivenza nell'Infarto Miocardico-3 Echo Substudy Investigators. Heterogeneity of left ventricular remodeling after acute myocardial infarction: results of the Gruppo Italiano per lo Studio della Sopravvivenza nell'Infarto Miocardico-3 echo substudy. Am Heart J 2001;141:131–8.
6. Davidoff R, Picard MH, Force T, et al. Spatial and temporal variability in the pattern of recovery of ventricular geometry and function after acute occlusion and reperfusion. Am Heart J 1994;127:1231–41.
7. Mann DL, Bristow MR. Mechanisms and models in heart failure. The biomechanical model and beyond. Circulation 2005;111:2837–49.
8. Lamas GA, Mitchell GF, Flaker GC, et al. Clinical significance of mitral regurgitation after acute myocardial infarction. Circulation 1997;96:827–33.
9. White HD, Norris RM, Brown MA, Brandt PW, Whitlock RM, Wild CJ. Left ventricular end-systolic volume as the major determinant of survival after recovery from myocardial infarction. Circulation 1987;76:44–51.
10. Otsuji Y, Handschumacher MD, Schwammethal E, et al. Insights from three-dimensional echocardiography into the mechanisms of functional mitral regurgitation: direct in vivo demonstration of altered leaflet geometry. Circulation 1997;96:1999–2008.
11. Cochran RP, Kunzelman KS. Effect of papillary muscle position on mitral valve function: relationship to homografts. Ann Thorac Surg 1998;66:S155–61.
12. Kaul S, Spotnitz WD, Glasheen WP, Touchstone DA. Mechanism of ischemic mitral regurgitation: an experimental evaluation. Circulation 1991;84:2167–80.
13. Lehmann KG, Francis CK, Dodge HT, the TIMI Study Group. Mitral regurgitation in early myocardial infarction: incidence, clinical detection and prognostic implications. Ann Intern Med 1992;117:10–7.
14. Grigioni F, Enriquez-Sarano M, Zehr KJ, Bailey KR, Tajik AJ. Ischemic mitral regurgitation: long-term outcome and prognostic implications with quantitative Doppler assessment. Circulation 2001;103:1759–64.
15. Carabello BA, Nakano K, Corin W, Biederman R, Spann JF Jr. Left ventricular function in experimental volume overload hypertrophy. Am J Physiol 1989;256:H974–81.
16. Urabe Y, Mann DL, Kent RL, et al. Cellular and ventricular contractile dysfunction in experimental canine mitral regurgitation. Circ Res 1992;70:131–47.
17. Ishihara K, Zile MR, Kanazawa S, et al. Left ventricular mechanics and myocyte function after correction of experimental chronic mitral regurgitation by combined mitral valve replacement and preservation of the native mitral valve apparatus. Circulation 1992;86:16–25.
18. Spinale FG, Ishihra K, Zile MR, DeFryte G, Crawford FA, Carabello BA. Structural basis for changes in left ventricular function and

geometry because of chronic mitral regurgitation and after correction of volume overload. J Thorac Cardiovasc Surg 1993;106:1147–57.
19. Ling LH, Enriquez-Sarano M, Seward JB, et al. Clinical outcome of mitral regurgitation due to flail leaflet. N Engl J Med 1996;335: 1417–23.
20. Guy TS, Moainie SL, Gorman JH, et al. Prevention of ischemic mitral regurgitation does not influence the outcome of remodeling after posterolateral myocardial infarction. J Am Coll Cardiol 2004;43: 377–83.
21. Carabello BA. Ischemic mitral regurgitation and ventricular remodeling. J Am Coll Cardiol 2004;43:384–5.
22. Trichon BH, Glower DD, Shaw LK, et al. Survival after coronary revascularization, with and without mitral valve surgery, in patients with ischemic mitral regurgitation. Circulation 2003;108 Suppl 1: 103–10.
23. Neskovic AN, Marinkovic J, Bojic M, Popovic AD. Early mitral regurgitation after acute myocardial infarction does not contribute to subsequent left ventricular remodeling. Clin Cardiol 1999;22:91–4.
24. Oh JH, Badhwar V, Mott BD, Li CM, Chiu RC. The effects of prosthetic cardiac binding and adynamic cardiomyoplasty in a model of dilated cardiomyopathy. J Thorac Cardiovasc Surg 1998;116:148–53.
25. Kelley ST, Malekan R, Gorman JH III, et al. Restraining infarct expansion preserves left ventricular geometry and function after acute anteroapical infarction. Circulation 1999;99:135–42.
26. Hung J, Guerrero JL, Handschumacher MD, Supple G, Sullivan S, Levine RA. Reverse ventricular remodeling reduces ischemic mitral regurgitation: echo-guided device application in the beating heart. Circulation 2002;106:2594–600.
27. Moainie SL, Guy TS, Gorman JH, et al. Infarct restraint attenuates remodeling and reduces chronic ischemic mitral regurgitation after postero-lateral infarction. Ann Thorac Surg 2002;74:444–9.
28. Llaneras MR, Nance ML, Streicher JT, et al. Large animal model of ischemic mitral regurgitation. Ann Thorac Surg 1994;57:432–9.
29. Rankin JS, Nicholas LM, Kouchoukos NT. Experimental mitral regurgitation: effects on left ventricular function before and after elimination of chronic regurgitation in the dog. J Thorac Cardiovasc Surg 1975;70:478–88.
30. Braunwald E, Welch GH Jr., Sarnoff SJ. Hemodynamic effects of quantitatively varied experimental mitral regurgitation. Circ Res 1957; 5:539–45.
31. Fisher JP, Picard MH, Mikan JS, et al. Quantitation of myocardial dysfunction in ischemic heart disease by echocardiographic endocardial surface mapping: correlation with hemodynamic status. Am Heart J 1995;129:1114–21.
32. Cheng W, Kajstura J, Nitahara JA, et al. Programmed myocyte cell death affects the viable myocardium after infarction in rats. Exp Cell Res 1996;226:316–27.
33. Foo RS, Mani K, Kitsis RN. Death begets failure in the heart. J Clin Invest 2005;115:565–71.
34. Wencker D, Chandra M, Nguyen K, et al. A mechanistic role for cardiac myocyte apoptosis in heart failure. J Clin Invest 2003;111: 1497–504.
35. Spinale FG, Coker ML, Heung LJ, et al. A matrix metalloproteinase induction/activation system exists in the human left ventricular myocardium and is upregulated in heart failure. Circulation 2000;102: 1944–9.
36. Sabbah HN, Sharov VG, Gupta RC, et al. Reversal of chronic molecular and cellular abnormalities due to heart failure by passive mechanical ventricular containment. Circ Res 2003;93:1095–101.
37. Zoghbi WA, Enriquez-Sarano M, Foster E, et al. Recommendations for evaluation of the severity of native valvular regurgitation with two-dimensional and Doppler echocardiography. J Am Soc Echocardiogr 2003;16:777–82.
38. Gorman JH, Gorman RC, Plappert T, et al. Infarct size and location determine development of mitral regurgitation in the sheep model. J Thorac Cardiovasc Surg 1998;115:615–22.
39. Young AA, Orr R, Smaill BH, Dell'Italia LJ. Three-dimensional changes in left and right ventricular geometry in chronic mitral regurgitation. Am J Physiol 1996;271:H2689–700.
40. Handschumacher MD, Lethor J-P, Siu SC, et al. A new integrated system for three-dimensional echocardiographic reconstruction: development and validation for ventricular volume with application in human subjects. J Am Coll Cardiol 1993;21:743–53.
41. Buck T, Handschumacher MD, Tanabe H, Guerrero JL, Levine RA. A new method for automatic quantification and visualization of regional left ventricular dysfunction by three-dimensional echocardiography: direct in vivo validation against three-dimensional sonomicrometry (abstr). J Am Coll Cardiol 1999;33:440A.
42. Mitchell GF, Lamas GA, Vaughan DE, Pfeffer MA. Left ventricular remodeling in the year after first anterior myocardial infarction: a quantitative analysis of contractile segment lengths and ventricular shape. J Am Coll Cardiol 1992;19:1136–44.
43. Nakano K, Swindle MM, Spinale FG, et al. Depressed contractile function due to canine mitral regurgitation improves after correction of the volume overload. J Clin Invest 1991;87:2153–61.
44. Glower DD, Spratt JA, Snow ND, et al. Linearity of the Frank-Starling relationship in the intact heart: the concept of preload recruitable stroke work. Circulation 1985;71:994–1009.
45. del Monte F, O'Gara P, Poole-Wilson PA, Yacoub M, Harding SE. Cell geometry and contractile abnormalities of myocytes from failing human left ventricle. Cardiovasc Res 1995;30:281–90.
46. del Monte F, Harding SE, Schmidt U, et al. Restoration of contractile function in isolated cardiomyocytes from failing human hearts by gene transfer of SERCA2a. Circulation 1999;100:2308–11.
47. Chu A, Dixon MC, Saito A, Seiler S, Fleischer S. Isolation of sarcoplasmic reticulum fractions referable to longitudinal tubules and junctional terminal cisternae from rabbit skeletal muscle. Methods Enzymol 1988;157:36–46.
48. Molkentin JD, Dorn GW II. Cytoplasmic signaling pathways that regulate cardiac hypertrophy. Annu Rev Physiol 2001;63:391–426.
49. Haq S, Choukroun G, Lim HW, et al. Differential activation of signal transduction pathways in human hearts with hypertrophy versus advanced heart failure. Circulation 2001;103:670–7.
50. Hirota H, Yoshida K, Kishimoto T, Taga T. Continuous activation of gp130, a signal-transducing receptor component for interleukin 6-related cytokines, causes myocardial hypertrophy in mice. Proc Natl Acad Sci U S A 1995;92:4862–6.
51. Communal C, Sumandea M, de Tombe P, Narula J, Solaro RJ, Hajjar RJ. Functional consequences of caspase activation in cardiac myocytes. Proc Natl Acad Sci U S A 2002;99:6252–6.
52. Spinale FG, Coker ML, Thomas CV, Walker JD, Mukherjee R, Hebbar L. Time-dependent changes in matrix metalloproteinase activity and expression during the progression of congestive heart failure: relation to ventricular and myocyte function. Circ Res 1998; 82:482–95.
53. Sam F, Sawyer DB, Chang DLF, et al. Progressive left ventricular remodeling and apoptosis late after myocardial infarction in mouse heart. Am J Physiol 2000;279:H422–8.
54. Rumberger JA. Ventricular dilatation and remodeling after myocardial infarction. Mayo Clin Proc 1994;69:664–74.
55. Levin HR, Oz MC, Chen JM, Packer M, Rose EA, Burkhoff D. Reversal of chronic ventricular dilation in patients with end-stage cardiomyopathy by prolonged mechanical unloading. Circulation 1995;91:2717–20.
56. Heerdt PM, Holmes JW, Cai B, et al. Chronic unloading by left ventricular assist device reverses contractile dysfunction and alters gene expression in end-stage heart failure. Circulation 2000;102:2713–9.
57. Ono K, Matsumori A, Shioi T, Furukawa Y, Sasayama S. Cytokine gene expression after myocardial infarction in rat hearts: possible implication in left ventricular remodeling. Circulation 1998;98:149–56.
58. Wollert KC, Taga T, Saito M, et al. Cardiotrophin-1 activates a distinct form of cardiac muscle cell hypertrophy. J Biol Chem 1996;271:9535–45.
59. Sivasubramanian N, Coker ML, Kurrelmeyer KM, et al. Left ventricular remodeling in transgenic mice with cardiac restricted overexpression of tumor necrosis factor. Circulation 2001;104:826–31.
60. MacKenna D, Summerour SR, Villarreal FJ. Role of mechanical factors in modulating cardiac fibroblast function and extracellular matrix synthesis. Cardiovasc Res 2000;46:257–63.
61. Kim HE, Dalal SS, Young E, Legato MJ, Weisfeldt ML, D'Armiento J. Disruption of the myocardial extracellular matrix leads to cardiac dysfunction. J Clin Invest 2000;106:857–66.
62. Coker ML, Thomas CV, Clair MJ, et al. Myocardial matrix metalloproteinase activity and abundance with congestive heart failure. Am J Physiol 1998;274:H1516–23.

63. Peterson JT, Hallak H, Johnson L, et al. Matrix metalloproteinase inhibition attenuates left ventricular remodeling and dysfunction in a rat model of progressive heart failure. Circulation 2001;103:2303–9.
64. Corin WJ, Monrad ES, Murakami T, Nonogi H, Hess OM, Krayenbuehl HP. The relationship of afterload to ejection performance in chronic mitral regurgitation. Circulation 1987;76:59–67.
65. Zile MR, Gaasch WH, Levine HT. Left ventricular stress-dimension-shortening relations before and after correction of chronic aortic and mitral regurgitation. Am J Cardiol 1985;56:99.
66. Dell'Italia LJ, Meng QC, Balcells E, et al. Increased ACE and chymase-like activity in cardiac tissue of dogs with chronic mitral regurgitation. Am J Physiol 1995;269:H2065–73.
67. Kapadia SR, Yakoob K, Nader S, Thomas JD, Mann DL, Griffin BP. Elevated circulating levels of serum tumor necrosis factor-alpha in patients with hemodynamically significant pressure and volume overload. J Am Coll Cardiol 2000;36:208–12.
68. Talwar S, Squire IB, Davies JE, Ng LL. The effect of valvular regurgitation on plasma cardiotrophin-1 in patients with normal left ventricular systolic function. Eur J Heart Fail 2000;2:387–91.
69. Otsuji Y, Handschumacher MD, Liel-Cohen N, et al. Mechanism of ischemic mitral regurgitation with segmental left ventricular dysfunction: three-dimensional echocardiographic studies in models of acute and chronic progressive regurgitation. J Am Coll Cardiol 2001;37:641–8.
70. Liel-Cohen N, Guerrero JL, Otsuji Y, et al. Design of a new surgical approach for ventricular remodeling to relieve ischemic mitral regurgitation. Circulation 2000;101:2756–63.
71. Hung J, Papakostas L, Tahta SA, et al. Mechanism of recurrent ischemic mitral regurgitation post-annuloplasty: continued LV remodeling as a moving target. Circulation 2004;110:85–90.
72. Enriquez-Sarano M, Avierinos JF, Messika-Zeitoun D, et al. Quantitative determinants of the outcome of asymptomatic mitral regurgitation. N Engl J Med 2005;352:875–83.
73. Kunisada K, Tone E, Fujio Y, Matsui H, Yamauchi-Takihara K, Kishimoto T. Activation of gp130 transduces hypertrophic signals via STAT3 in cardiac myocytes. Circulation 1998;98:346–52.
74. Hirota H, Chen J, Betz UAK, et al. Loss of a gp130 cardiac muscle cell survival pathway is a critical event in the onset of heart failure during biomechanical stress. Cell 1999;97:189–98.
75. Zolk O, Ng LL, O'Brien RJ, Weyand M, Eschenhagen T. Augmented expression of cardiotrophin-1 in failing human hearts is accompanied by diminished glycoprotein 130 receptor protein abundance. Circulation 2002;106:1430–2.
76. Craig R, Wagner M, McCardle T, Craig AG, Glembotski CC. The cytoprotective effects of the glycoprotein 130 receptor-coupled cytokine, cardiotrophin-1, require activation of NF-kappa B. J Biol Chem 2001;276:37621–9.
77. Shioi T, Kang PM, Douglas PS, et al. The conserved phosphoinositide 3-kinase pathway determines heart size in mice. EMBO J 2000;19:2537–48.
78. Matsui T, Tao J, del Monte F, et al. Akt activation preserves cardiac function and prevents injury after transient cardiac ischemia in vivo. Circulation 2001;104:330–5.
79. Rosen BD, Edvardsen T, Lai S, et al. Left ventricular concentric remodeling is associated with decreased global and regional systolic function. The Multi-Ethnic Study of Atherosclerosis. Circulation 2005;112:984–91.
80. Drazner MH. The transition from hypertrophy to failure: how certain are we? Circulation 2005;112:936–8.
81. Spinale FG, Coker ML, Bond BR, Zellner JL. Myocardial matrix degradation and metalloproteinase activation in the failing heart: a potential therapeutic target. Cardiovasc Res 2000;46:225–38.
82. Cheng A, Nguyen TC, Malinowski M, et al. Effects of undersized mitral annuloplasty on regional transmural left ventricular wall strains and wall thickening mechanisms. Circulation 2006;114:I600–9.
83. Wu AH, Aaronson KD, Bolling SF, Pagani FD, Welch K, Koelling TM. Impact of mitral valve annuloplasty on mortality risk in patients with mitral regurgitation and left ventricular systolic dysfunction. J Am Coll Cardiol 2005;45:381–7.